

## Testing an optical window of a small wedge angle

Chiayu Ai and James C. Wyant

WYKO Corporation, 2650 E. Elvira Road, Tucson, Arizona 85706

### ABSTRACT

Multiple reflections between two surfaces of a window introduce a fixed pattern error in the transmitted wavefront. In a Fizeau or Twyman-Green interferometer, this wavefront is reflected by a return flat and transmits through the window. The fixed pattern error is carried in the measurement result. This error is negligible, only if the wedge angle is so large that the interference fringes formed by the two surfaces are too dense for the detector to resolve. However, if the wedge angle is small (e.g. several arc-seconds), the phase error (pv) could be up to 0.025 fringes for most glass ( $n = 1.5$ ). By tilting both the window and the return flat properly, it is possible to cancel the effect of multiple reflections of a window.

### 2. THEORY

Spurious reflections usually introduce errors into the measurement results obtained with laser phase-shifting interferometry.<sup>1-7</sup> For a Fizeau interferometer, work has been done to reduce or eliminate the effect of the multiple reflections between the test and reference surfaces. For example, Hariharan<sup>3</sup> points out that if a four-frame phase calculation algorithm is used, the phase error caused by multiple reflections is eliminated to a first order approximation. Bonsch and Bohme<sup>5</sup> give a new algorithm which can completely eliminate the phase error due to multiple reflections of a test mirror.

For a planar parallel plate or optical window, the relative amplitudes of the successive internally reflected rays are  $1, r^2, r^4, \dots$ , where  $r$  is the coefficient of reflection of the window. If the incident angle is  $\theta$ , it can be shown that the optical path difference (OPD) of two successive rays is equal to  $2dn \cos(\theta')$ , where  $d$  and  $n$  are the thickness and the refractive index of the window, respectively, and  $\theta'$  is the refractive angle. The coefficient of reflection,  $r$ , of most optical glass is about 20%. Therefore the multiple reflections of a window can be approximated by the first two rays, i.e.,  $1$  and  $r^2$ . These two rays are reflected back to the window by the return flat (RF), whose coefficient of reflection is  $s$ , as shown in Fig. 1. Between the window and the RF, the filled-arrow ray has a relative amplitude of  $s$ , and the open-arrow ray has a relative amplitude of  $r^2s$ . Each of the two rays reflected by the RF has multiple reflections inside the window. The multiple reflections of the filled-arrow ray in the window can be approximated by the first two rays,  $E_t$  and  $E_{g2}$ . Because of the low reflectivity of the window, the multiple reflections of the open-arrow ray in the window are negligible; only the transmitted ray  $E_{g1}$  is significant. Therefore for an incident ray from the source entering the window, there are three returned rays,  $E_t$ ,  $E_{g1}$ , and  $E_{g2}$ , as shown in Fig. 1. Because of the non-zero incident angle, the returned rays  $E_{g1}$  and  $E_{g2}$  are laterally displaced from the original incident location approximately by  $d\theta(1 - 1/n)$ , and go through different regions of the window,  $x_1$  and  $x_2$ , respectively. If the thicknesses of the two regions are  $d(x_1, y)$  and  $d(x_2, y)$ , respectively, the complex amplitudes of the rays are

$$\begin{aligned}
E_t &= s \exp i[2\phi_w(x,y) + \phi_r(x,y)], \\
E_{g1} &= r^2 s \exp i[\phi_w(x,y) + \phi_w(x_1,y) + \phi_r(x,y) + 2d(x_1,y)n \cos(\theta')k], \\
E_{g2} &= r^2 s \exp i[\phi_w(x,y) + \phi_w(x_2,y) + \phi_r(x,y) + 2d(x_2,y)n \cos(\theta')k],
\end{aligned} \tag{1}$$

where  $k = 2\pi/\lambda$ , and  $\theta'$  is the refracted angle inside the window. The  $\phi_w(x,y)$  and  $\phi_r(x,y)$  are the contributions of the window and the RF, respectively. For a small wedge angle, the displacement is negligible, i.e.,  $x_1 \approx x_2$ . In Fig. 1, the RF is not tilted, and hence  $x_1 \approx x_2 \approx x$ . Because of the wedge angle, the optical thickness  $d(x,y)n$  is not equal to a constant over the window. The phase of vector sum of the three rays is a function of  $d(x,y)n$  with a period of  $1\lambda$ . Because the vector sum of the three rays varies with the optical thickness of a window along its wedge direction, the resulting wave front and the measurement result have ripples perpendicular to the wedge direction. In the following we show that the tilt of the return flat (RF) can alter the effect of the multiple reflections on the phase measurement.

If the RF is tilted at an angle  $\epsilon$ , the returned ray  $E_t$  deviates from the original location  $x$  to  $x'$  on the window. When both the window and the RF are tilted in the same direction, the incident angle of the returned ray is  $\theta - 2\epsilon$ . If they are tilted in the opposite direction, then the incident angle is  $\theta + 2\epsilon$ , as shown in Fig. 2. Since the three returned rays are close to each other, we use  $x'$  to represent their locations on the window, and the distance of  $x' - x$  is defined as the walk-off distance. For simplicity, we assume that the lateral displacement due to refraction is smaller than the walk-off distance. Therefore, the OPD between  $E_t$  and  $E_{g2}$  is equal to  $2d(x',y)n \cos(\theta'')$ , where  $\theta''$  is the corresponding refracted angle for the incident angle of either  $\theta - 2\epsilon$  or  $\theta + 2\epsilon$ , depending on the tilt directions. The complex amplitudes of the three returned rays are

$$\begin{aligned}
E_t &= s \exp i[\phi_w(x,y) + \phi_w(x',y) + \phi_r(x,y)], \\
E_{g1} &= r^2 s \exp i[\phi_w(x,y) + \phi_w(x',y) + \phi_r(x,y) + 2d(x,y)n \cos(\theta')k], \\
E_{g2} &= r^2 s \exp i[\phi_w(x,y) + \phi_w(x',y) + \phi_r(x,y) + 2d(x',y)n \cos(\theta'')k].
\end{aligned} \tag{2}$$

It should be noted that for  $E_{g1}$  the multiple reflections occur at  $x$  not  $x'$ , and hence the OPD between  $E_t$  and  $E_{g1}$  is equal to  $2d(x,y)n \cos(\theta')$ , not  $2d(x',y)n \cos(\theta'')$ . Mainly due to the change in the incident angle, the value of  $2d(x',y)n \cos(\theta'')$  is different from that of  $2d(x,y)n \cos(\theta')$ . This makes it possible to cancel  $E_{g1}$  with  $E_{g2}$  and eliminate the effect of multiple reflections.

For convenience, we define a quantity  $\varphi$  as the angle between  $E_{g1}$  and  $E_{g2}$ , and  $L$  as the magnitude of the sum phasor,  $E_{g1} + E_{g2}$ . Because  $E_{g1}$  and  $E_{g2}$  have the same magnitude,  $\varphi$  and  $L$  can be expressed as follows,

$$\begin{aligned}
\varphi &= 2d(x,y)n \cos(\theta')k - 2d(x',y)n \cos(\theta'')k, \\
L &= 2r^2 s |\cos(\varphi/2)|.
\end{aligned} \tag{3}$$

For a given  $L$ , the two extremes of the errors are  $\pm \sin^{-1}(L/|E_t|)$  in radians. Therefore

$$\begin{aligned} \text{Phase error (pv)} &= 2 |\sin^{-1}[2r^2\cos(\varphi/2)]| && \text{in radians} \\ &= |\sin^{-1}[2r^2\cos(\varphi/2)]|/\pi. && \text{in fringes} \end{aligned} \quad (4)$$

From Eqs. (3) and (4), when  $\varphi = \text{odd}\pi$ , both  $L$  and the error are zero. When  $\varphi = \text{even}\pi$ , both  $L$  and the error are maximum. If the coefficient of the reflection is about 20%, i.e.  $r^2 = 4\%$ , then the phase error (pv) = 0.0254 fringe. For simplicity, we assume that the walk-off is negligible or the window has an equal thickness in the direction of the walk-off, e.g., the  $x$ -direction. Hence  $d(x,y) = d(x',y) = d$ , and

$$\varphi = 2dk \{ [1 - \sin^2(\theta)/n^2]^{1/2} - [1 - \sin^2(\theta - 2\varepsilon)/n^2]^{1/2} \}, \quad (5)$$

$$\varphi \approx 4dk\theta\varepsilon/n, \quad \text{if } \varepsilon \ll \theta \ll 1, \quad (6)$$

$$\varphi \approx 2dk(2\theta - \varepsilon)\varepsilon/n, \quad \text{if } \varepsilon \approx \theta \ll 1. \quad (6a)$$

It is important to note that because the term in the curved bracket is a very small number, the angle  $\varphi$  is not sensitive to  $d$ , but is very sensitive to  $\varepsilon$  and  $\theta$ . From Eq. (5), the values of  $\varphi$ ,  $L$ , and phase error (in fringes) are listed in the table below for different tilt angles  $\theta$  and  $\varepsilon$ , where  $n = 1.5$ ,  $\lambda = 633$  nm, and  $d = 10$  or  $20$  mm.

$\theta$	$\varepsilon$ (d = 10 mm)	$\varepsilon$ (d = 20 mm)	$\varphi$	$L$	Phase error (pv)
$x$	$0^\circ$	$0^\circ$	0	$2r^2s$	0.0254
$0.5^\circ$	$0.06853^\circ$	$0.03633^\circ$	$\pi$	0	0
$0.5^\circ$	$0.12474^\circ$	$0.06853^\circ$	$2\pi$	$2r^2s$	0.0254
$1^\circ$	$0.03756^\circ$	$0.01912^\circ$	$\pi$	0	0
$1^\circ$	$0.07266^\circ$	$0.03756^\circ$	$2\pi$	$2r^2s$	0.0254
$2^\circ$	$0.01930^\circ$	$0.00970^\circ$	$\pi$	0	0
$2^\circ$	$0.03825^\circ$	$0.01931^\circ$	$2\pi$	$2r^2s$	0.0254

If  $\varepsilon \neq 0^\circ$ ,  $\varphi$  can be any values according to Eq. (5). For a given  $\theta$  and  $\varepsilon$ , a slight increment in the window thickness, e.g.,  $\Delta d = 2\lambda$ , increases the OPD between two successive internally reflected rays by  $2\Delta dn$ , i.e.,  $6\lambda$ . The angle of each phasor  $E_{g1}$  and  $E_{g2}$  increases by  $12\pi$  for  $n = 1.5$ . Because the angles of both phasors  $E_{g1}$  and  $E_{g2}$  increase by the same amount, the angle of the sum phasor also increases  $12\pi$ . But the angle  $\varphi$  between the two phasors does not vary with the  $y$ -direction, and remains unchanged. For example, a window has an equal thickness in the  $x$ -direction and a wedge of  $2\lambda$  in the  $y$ -direction. If this window is tilted in the  $x$ -direction, then the angle of the sum phasor  $E_{g1} + E_{g2}$  varies with the  $y$ -direction by  $12\pi$ . Therefore if  $\varphi \neq \text{odd}\pi$ , then the resulting wave front shows six horizontal fringes, i.e. a ripple of six cycles in the  $y$ -direction. If the RF is tilted such that  $\varphi = \text{odd}\pi$ , then  $E_{g1}$  and  $E_{g2}$  cancel each other, as if there were no multiple reflections. For the same wedge window, whenever  $\varepsilon = 0^\circ$ ,  $\varphi$  always equals

zero, regardless of the tilt and the thickness of the window, and the resulting wave front shows a ripple of six cycles in the y-direction.

The condition of  $\varphi = m\pi$  is important for minimizing ( $m = \text{odd}$ ) or maximizing ( $m = \text{even}$ ) the effect of multiple reflections. Because  $\varepsilon \ll \theta \ll 1$  in most cases, from Eq. (6) and the condition of  $\varphi = m\pi$ , we obtain  $4dk\theta\varepsilon/n = m\pi$ , where  $\theta$  and  $\varepsilon$  are in radians. Therefore the phase error is either minimum ( $\approx 0$ ) or maximum ( $p_v \approx 2r^2/\pi$ , in fringes) when one of the following conditions is satisfied.

$$\text{Phase error is minimum, if } d\theta^\circ\varepsilon^\circ/\lambda n \approx m \times 0.000406 \text{ and } m = \text{odd}, \quad (7)$$

$$\text{Phase error is maximum, if } d\theta^\circ\varepsilon^\circ/\lambda n \approx m \times 0.000406 \text{ and } m = \text{even}, \quad (8)$$

where  $\theta^\circ$  and  $\varepsilon^\circ$  are equivalent to  $\theta$  and  $\varepsilon$  in degrees,  $d$  is in mm,  $\lambda$  is in nm, and  $r$  is the coefficient of reflection. From Eqs. (7) and (8), if  $n = 1.5$  and  $\lambda = 633$  nm, then

$$d\theta^\circ\varepsilon^\circ \approx 0.386m, \quad (9)$$

where  $m$  is a natural number. The results of this equation for  $m = 1$  and  $2$  correspond to those in the table above for  $\varphi = \pi$  and  $2\pi$ , respectively. This equation is very useful for estimating the proper tilt angles for the window and the RF.

### 3. EXPERIMENT

In the experiment, a laser phase-shifting Fizeau interferometer is used. A window of a BK7 plate (20 mm thick and 150 mm in diameter, with a wedge angle of 1.725 arc-seconds) is placed between the RF and transmission flat (TF). If this wedge is oriented in the vertical direction, it can be shown that this window introduces six horizontal fringes in the transmitted wave front. First, we look at the intensity pattern of the sum of the three returned rays,  $E_t + E_{g1} + E_{g2}$ , by removing the TF from the interferometer. The window is tilted such that no direct reflections from the front and the rear surfaces of the window enter the detector. The tilt direction of the window can be categorized into two cases: (A) the window tilt direction is perpendicular to the window wedge direction, and (B) the window tilt direction is parallel to the window wedge direction. For convenience, we orient the window such that the wedge is in the y-direction, and it is either tilted in the x-direction or in the y-direction. For Case (A), the window is tilted  $\theta = 0.5^\circ$  in the x-direction. Figure 3 shows the intensity pattern, when the RF is not tilted,  $\varepsilon = 0^\circ$ . The intensity pattern has faint but obvious horizontal interference (ghost) fringes. When the RF is tilted in the x-direction,  $\varepsilon = 0.03633^\circ$ , from the table above we obtain  $\varphi = \pi$ , and hence the ghost fringes disappear. Increasing the tilt of the RF to  $0.06853^\circ$ , these ghost fringes reappear. In Case (B), the window is tilted in the y-direction ( $\theta = 0.5^\circ$ ), i.e., the window tilt direction is parallel to the window wedge direction. When the RF is tilted in the y-direction,  $\varepsilon = 0.03633^\circ$ , the ghost fringes disappear. Therefore, as long as the RF is tilted in the same plane as that for the tilt of the

window, the interference ghost fringes can disappear easily, regardless of the window wedge direction. On the other hand, whenever  $\varepsilon = 0^\circ$ , the interference ghost fringes cannot be removed.

To measure the phase of the resulting wave front of the three return rays,  $E_t + E_{g1} + E_{g2}$ , the TF is put back into the interferometer and tilted to give several vertical fringes. Figure 4 shows the intensity patterns for the same window used in Fig. 3, when the RF is (a) not tilted or (b) tilted in the x-direction,  $\varepsilon = 0.03633^\circ$ , respectively. The wedge is in the y-direction, and the window is tilted  $0.5^\circ$  in the x-direction. In Fig. 4a, when the RF is not tilted, there are several vertical main fringes and six ghost horizontal fringes which are the same as those in Fig. 3. When the RF is tilted  $0.03633^\circ$  in the x-direction, the ghost fringes disappear as shown in Fig. 4b. Figure 5 is the measured wave front obtained from the interferograms in Fig. 4. In Fig. 5a, the ripples correspond to the ghost fringes in Figs. 3 and 4a. The ripples have the phase error (pv)  $\approx 0.025 \lambda$ .

Figure 6a shows the intensity distribution of a  $120 \times 120 \times 3$  mm thin fused silica plate. It is obtained using the same interferometer without a TF, when the RF is not tilted. There are several very curved ghost fringes which are a fixed pattern caused by the multiple reflections. It should be noted that these curved ghost fringes have a sharp bending around the boundary of the plate due to the rapid thickness variation at the edges. Removing the RF, we obtain the same intensity pattern in the transmitted beam. The ghost fringes shift very quickly whenever the tilt angle is changed. When the RF is replaced, but not tilted, to reflect the beam back into the interferometer, we obtain the same ghost fringe pattern. The ghost fringes may disappear when the RF is tilted properly, as shown in Fig. 6b.

#### 4. CONCLUSION

To effectively remove the ghost fringes, we propose the following procedure for a Fizeau interferometer. This procedure can also be applied to a Twyman-Green interferometer, where the reference mirror is equivalent to the TF.

- (1) Tilt the TF by a large angle to avoid the main interference fringes. Adjust the RF such that it is normal to the collimated beam.
- (2) Insert the window into the cavity and orient the wedge in one direction. Choose a proper tilt angle  $\theta$  for the window. Tilt the window at this angle in any direction. An intensity pattern with a faint interference pattern can be observed, such as in Fig. 3.
- (3) Tilt the RF in the same or opposite direction as that for the tilted window. The faint interference pattern in Step 2 disappears and then appears repeatedly when the tilt angle increases. The angle corresponding to the first disappearance of the interference pattern should be chosen because it introduces the smallest walk-off. This tilt angle corresponds to  $\varepsilon^\circ$  in Eq. (9) for  $m = 1$ .
- (4) Adjust the TF to form the main interference fringes.

When the fixed pattern has several fringes, the disappearance of the fringes in Step 3 is very obvious, and this procedure is easy to follow. However, if the wedge angle is so small and the surfaces are so flat that the ghost interference pattern is about one fringe or less in Step 2, then it might be difficult to observe the disappearance of the fringe in Step 3. In summary, when testing

an optical window, a collimated beam transmits through the window and then is reflected back by a return flat (RF). The window is always tilted and the incident angle to the window is not zero. If the RF is tilted slightly, the re-incident angle of the ray reflected by the RF is different from the original incident angle. Therefore, the multiple reflections related to these two incident angles are different, and the ghost fringes can be canceled. To effectively remove the ghost fringes, one needs to tilt the RF in the same plane as that for the tilt of the window, regardless of the window wedge direction. We have shown that the effect of multiple reflections of the window can be removed by tilting both the window and the RF properly. This method allows us to measure a window with a small wedge angle of several arc-seconds, without using antireflective coatings on both surfaces.

## 5. REFERENCES

1. J. H. Bruning, J. E. Gallagher, D. P. Rosenfeld, A. D. White, D. J. Brangaccio, and D. R. Herriott, "Digital wave front measuring interferometer for testing optical surfaces and lenses," *Appl. Opt.* **13**, 2693-2703 (1974).
2. J. Schwider, R. Burow, K.-E. Elssner, J. Grzanna, R. Spolaczyk, and K. Merkel, "Digital wave-front measuring interferometry: some systematic error sources," *Appl. Opt.* **22**, 3421-3432 (1983).
3. P. Hariharan, "Digital phase-stepping interferometry: effects of multiply reflected beams," *Appl. Opt.* **26**, 2506-2507 (1987).
4. C. Ai and J. C. Wyant, "Effect of spurious reflection on phase shift interferometry," *Appl. Opt.* **27**, 3039-3045 (1988).
5. G. Bonsch and H. Bohme, "Phase-determination of Fizeau interferences by phase-shifting interferometry," *Optik* **82**, 161-164 (1989).
6. R. A. Nicolaus, "Evaluation of Fizeau interferences by phase-shifting interferometry," *Optik* **87**, 23-26 (1991).
7. C. Ai and J. C. Wyant, "Effect of retroreflection on a Fizeau phase-shifting interferometer," *Appl. Opt.*, in press.

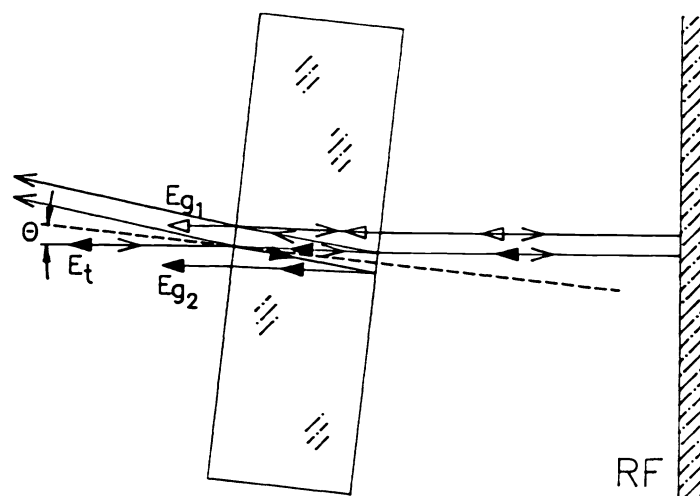


Fig. 1 Ray path through a window and reflected by a return flat (RF). The window is tilted at an angle  $\theta$ , but the RF is not tilted.

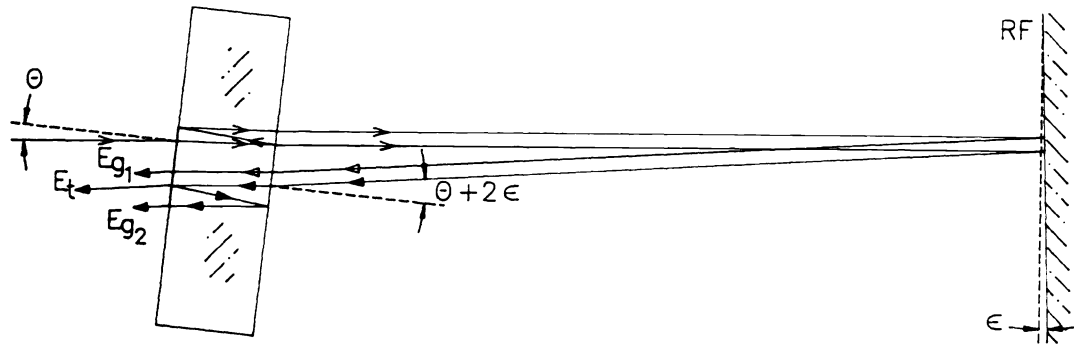


Fig. 2 Similar to Fig. 1, except the RF is tilted by an angle  $\epsilon$ . The reflected ray deviates from the original location. Here, the RF is away from the window to show the ray deviation. This deviation can be reduced by moving the RF closer to the window.

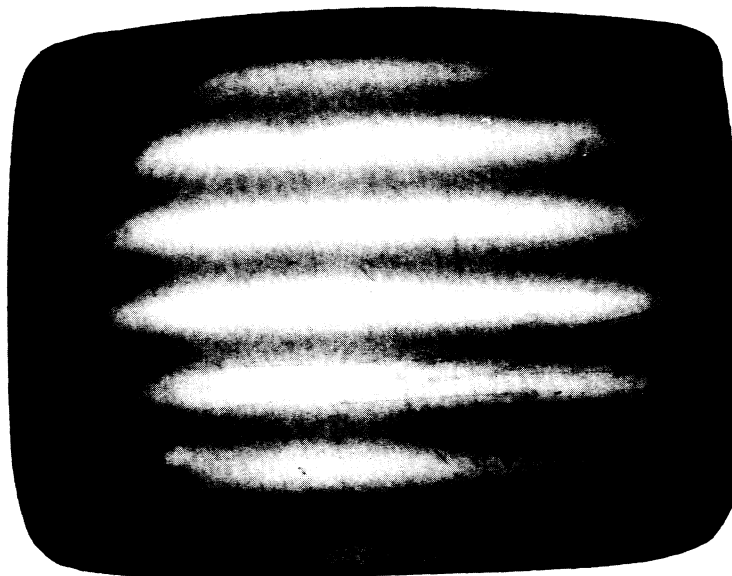


Fig. 3 Intensity pattern obtained with RF and a 20 mm thick BK7 window. The window has a wedge in the y-direction and is tilted in the x-direction ( $\theta = 0.5^\circ$ ), but the RF is not tilted.

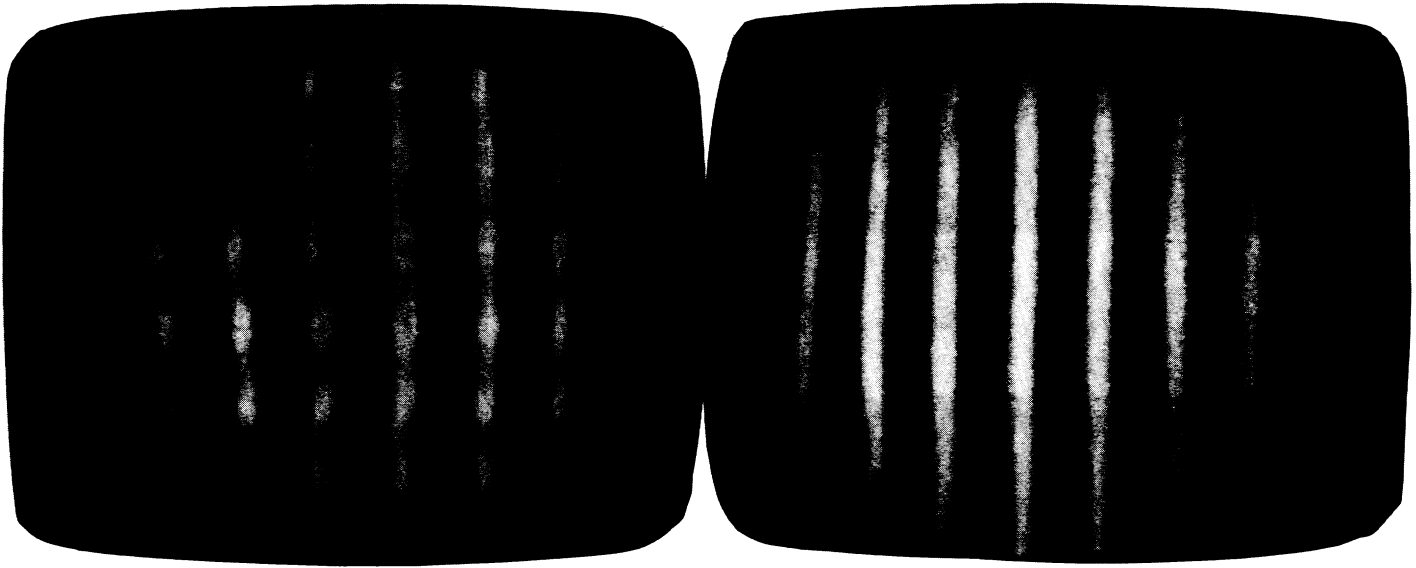
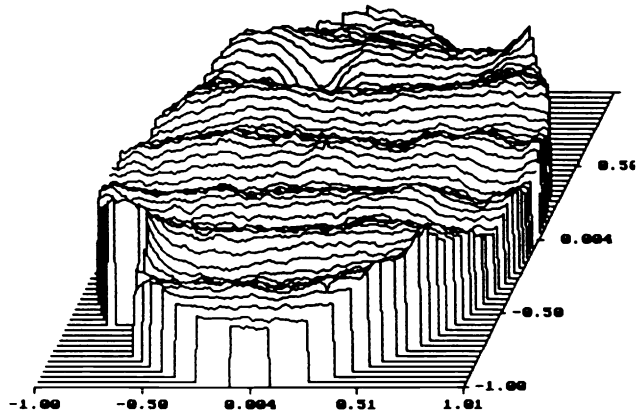


Fig. 4 Intensity patterns for the same window in Fig. 3, when the TF is tilted to give several vertical fringes. (a) The RF is not tilted, and (b) the RF is tilted properly.

PV: 0.191  $\mu\text{w}$   
 MV/FRN: 1.00

OPD



PV: 0.285  $\mu\text{w}$   
 MV/FRN: 1.00

OPD

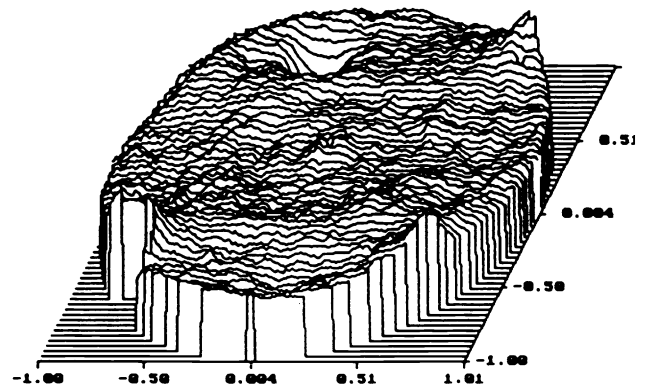


Fig. 5 Measured wave front obtained from Fig. 4. (a) The ripple  $\approx 0.025 \lambda$  (pv). (b) The ripple disappears.

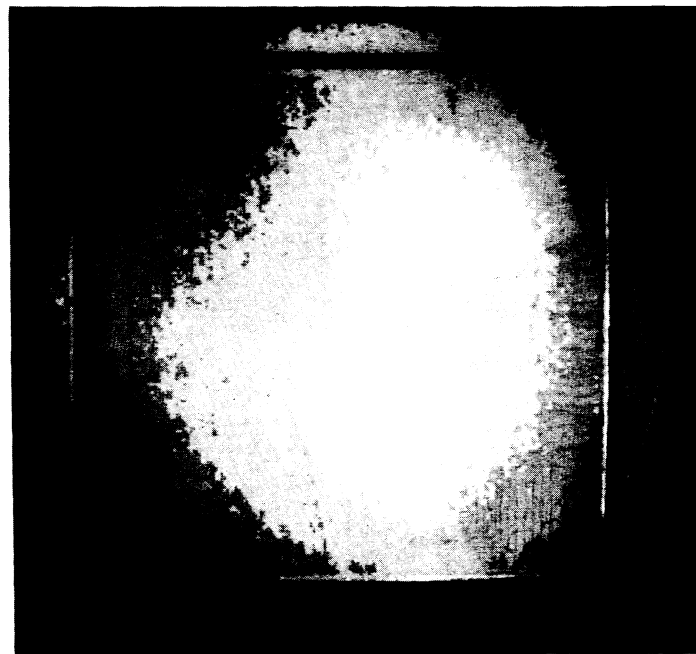
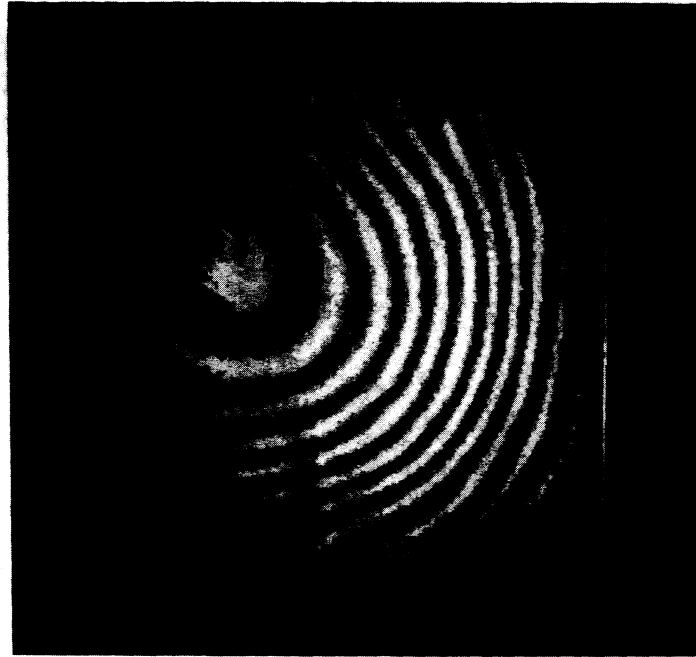


Fig. 6 Intensity patterns obtained with RF and a 3 mm thick fused silica window. (a) The RF is not tilted, and (b) the RF is tilted properly.